Theoretical and Applied Fracture Mechanics 86 (2016) 69–77

Contents lists available at ScienceDirect

Theoretical and Applied Fracture Mechanics

journal homepage: www.elsevier.com/locate/tafmec

The contribution of small punch testing towards the development of materials for aero-engine applications

Roger C. Hurst, Robert J. Lancaster *, Spencer P. Jeffs, Martin R. Bache

Swansea University, Institute of Structural Materials, Bay Campus, Fabian Way, Swansea SA1 8EN, United Kingdom

ARTICLE INFO

Article history:
Received 28 June 2016
Revised 28 July 2016
Accepted 28 July 2016
Available online 30 July 2016

Keywords:
Small punch
Review
Aero-engine materials

ABSTRACT

This paper, invited for presentation at the 33rd Meeting of the Spanish Group on Fracture and Structural Integrity, March 2016 in San Sebastian, Spain, reviews the recent work carried out in the authors' laboratory, addressing the elucidation of tensile and creep characteristics of materials for aero engine components. Two specific applications of the Small Punch (SP) test assessment technology were identified, the first of these takes on board the unique potential of the SP test for testing small quantities of materials which are either in development or through their directional structure cannot easily be produced in quantities which would allow conventional mechanical testing. This goal also required the development and procurement of new SP test facilities capable of operation up to 1150 °C. The examples given in this paper are TiAl intermetallic alloys and nickel based single crystals, all studied utilising the Code of Practice for SP Creep Testing. The second application illustrates the use of SP testing to assess both the tensile and creep properties of additive layer manufactured (ALM) alloys such as IN718 and Ti-6Al-4V using the Code of Practice for SP Tensile and Fracture Testing. Due to the unavailability of sufficient material to facilitate conventional testing for comparison of materials property data, SP testing is unable to provide absolute data for all of these applications, nevertheless the ranking capabilities of SP testing are demonstrably proven.

1. Introduction

In the 1980s the original intention of the Small Punch Test was to assess the degradation of nuclear reactor components as a result of irradiation damage [1,2]. This was mainly aimed at determining tensile and fracture properties of the reactor pressure vessel steels [3,4]. A decade later the technique was encouraged for application to study the degradation due to creep of conventional fossil fuel fired energy plant components [5]. Mainly for these two types of applications, a European Code of Practice (EUCoP) for SP tensile, fracture and creep testing was developed early in the 21st century and launched by CEN in 2006, revised in 2007 [6].

This rigid foundation for the methodology encouraged a major engagement by many laboratories, particularly in Europe, to exploit the technique further and extend to other industrial sectors. In particular, the aero-engine community have recognised the unique potential of the SP creep test for testing small quantities of novel candidate materials which cannot be produced in quantities which would allow significant conventional mechanical testing due to prohibitive cost. Here the continuous evolution of the jet engine has led to the need to develop new alloys to withstand the increasing temperatures experienced in service, providing a major challenge to materials scientists and engineers. Recent advances have led designers to re-evaluate the suitability of traditional alloy systems for high temperature components, particularly as operating temperatures approach the limitation of many currently employed nickel based superalloys. Although improved component design, advanced cooling procedures and thermal barrier coatings continue to ameliorate various issues, research into materials which are envisaged to replace established structural metallic systems for elevated temperature turbine disc and blade applications within a twenty year horizon, now constitutes a major research activity.

For the assessment of these novel candidate materials, either metallic or intermetallic in nature, the small punch (SP) test technique immediately serves as a cost effective, front-runner amongst presently available miniaturised test techniques. To date, the vast majority of interest in the SP technique has focussed on relatively ductile alloys. However, prior to the application of SP tests to potential new alloys, some of which may be brittle in nature at least at ambient temperature, a thorough assessment of the technique for an archetypal brittle alloy must be considered. As important as alloy development is the ability of SP testing to assess the

* Corresponding author.
E-mail address: r.j.lancaster@swansea.ac.uk (R.J. Lancaster).

http://dx.doi.org/10.1016/j.tafmec.2016.07.013
0167-8442/

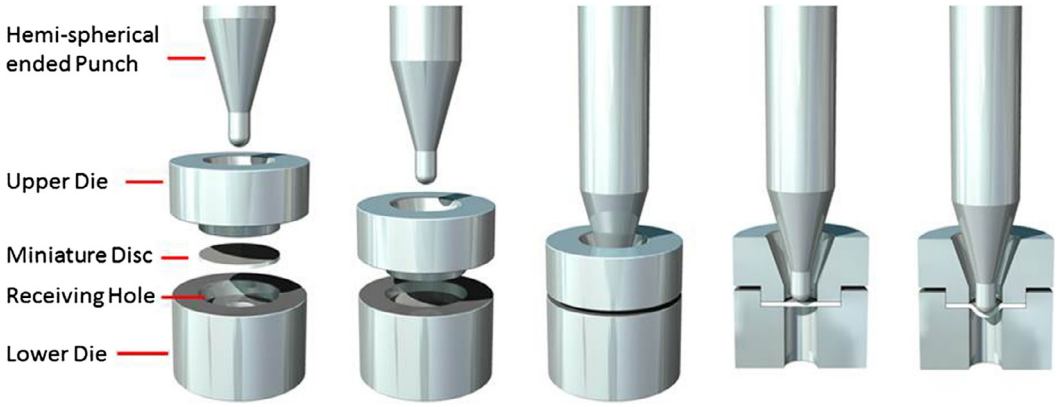

Fig. 1. Schematic representation of disc retention and punch application.

potential of the various techniques of additive layer manufacturing (ALM) aimed at gas turbine component repair and in the future for complete component manufacture. Here the advantage of being able to test small build volumes in tandem with process optimisation is complemented by the ability to assess mechanical properties in different orientations. This is also advantageous when characterising anisotropic materials such as single crystal alloys.

The present paper will serve to review the following four "case studies", selected examples from our recent research portfolio, where SP testing has been employed to address the range of requirements detailed above:

- CMSX-4® – an established single crystal turbine blade alloy, demonstrating notable directional mechanical properties.
- γTiAl – a brittle intermetallic at room temperature, intended for aerofoil applications in the low pressure turbine.
- IN718 – assessed as a developmental additive material for future aerofoil repair applications.
- Ti-6Al-4V – comparing conventional wrought and cast variants to novel electron beam melted material.

Throughout, evidence is provided to support the use of SP testing to define constitutive behaviour, demonstrating a sensitivity to microstructure and micro-texture variations, illustrating high temperature creep characteristics and correlations to conventional creep data.

2. Experimental approach

Two distinct small punch rig designs are required for (i) tensile and fracture testing and (ii) creep testing. However, both rely on loading a hemispherical ended punch or a recessed punch holding a spherical ball onto a thin disc specimen held in a clamped ring above a 4 mm receiving aperture, as displayed in Fig. 1. The deflection of the disc is continually monitored and is recorded against either increasing load under a constant rate of displacement in a tensile test or a constant applied load against time in a creep test. Tensile testing is usually conducted under higher loads than the creep test and a bespoke high temperature SP test jig has been designed for location within the load train of a universal, servo-actuated test frame. For higher temperature but lower load SP creep testing, a new free standing facility has been commissioned, which can operate at temperatures up to 1150 °C. The choice of punch material and diameter is determined by the loads required and test temperature. Normally, 2–2.5 mm diameter punches manufactured from Nimonic 90 are applied for tensile tests both at room and elevated temperature, with ceramic punches employed for very high loads and for creep tests at high temperatures. The other main difference between the equipment concerns the need for inert gas protection of the thin disc in the SP creep tests to resist oxidation under prolonged exposures. Depending upon the form of the as received stock material, discs are extracted using electrical discharge machining, then ground and polished to 500 μm ± 5 μm thickness. To reiterate, all testing was carried out according to the provisions set down in the EUCoP [6].

3. Results and discussion

3.1. Nickel based single crystals

Research has been completed to determine the suitability of the SP creep test when applied to single crystal forms of nickel based superalloy. The alloy selected was the established turbine blade alloy CMSX-4®,[1] tested at elevated temperatures of 950 °C, 1050 °C and 1150 °C. These temperatures in themselves mark a significant extension in SP capability when compared to the original intentions for SP techniques during the 1980s. The results were correlated with conventional uniaxial creep test approaches and used to demonstrate the implementation of long term lifing techniques to the relatively short term SP creep data. It is noteworthy that SP evaluation was capable of replicating the effects of microstructural evolution that prevails in this system across this temperature range.

It is inevitable that the characteristic, anisotropic nature of single crystal superalloys, where an improved creep response is found in a specific orientation, would influence the SP creep test. The biaxial stress distribution imposed during a SP creep test and the FCC unit cell of CMSX-4® are illustrated in Fig. 2. SP disc specimens were sectioned from a cylindrical rod of CMSX-4® grown in the ⟨0 0 1⟩ direction and therefore tested with load applied onto the orthogonal [1 0 0–0 1 0] plane.

Employing conventional, uniaxial creep testing, previous workers have demonstrated that under intermediate temperatures (700 °C) anisotropy is prominent in this alloy; crystals grown in the [0 0 1] orientation typically exhibited the strongest uni-axial creep resistance when stressed parallel to this orientation, followed by crystals loaded in the [0 1 1] orientation, with the [1 1 1] orientation demonstrating the weakest response. The strength effect is most pronounced during the primary creep phase [7,8]. However, at elevated temperatures, >980 °C, creep behaviour is seen to be far more isotropic. For example, at 1050 °C and 120 MPa, [0 0 1] orientated crystals exhibit a creep life between 468 and 705 h, [0 1 1] orientation a life of 536 h and [1 1 1] orien-

[1] ®CMSX-4 is a registered trademark of Cannon-Muskegon Corporation.

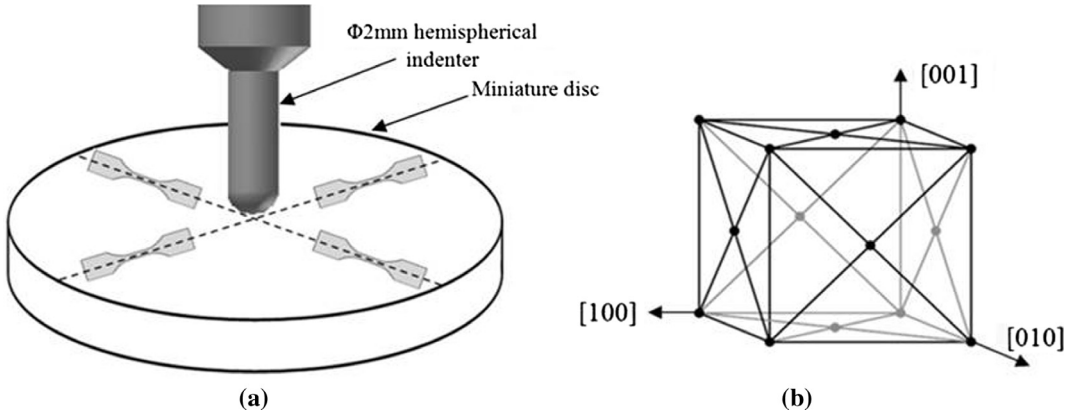

Fig. 2. Representation of (a) the biaxial tensile stress imposed on a SP creep specimen and (b) the corresponding FCC unit cell of CMSX-4® [12].

tated crystals a life of 474–682 h [1]. As a result, at these elevated temperatures the CMSX-4® material was considered isotropic. Note that the SP testing conducted by the current team was consistent with the previously defined high temperature, isotropic regime.

At these elevated temperatures, microstructural rafting occurs over a prolonged period of time, in which CMSX-4® can evolve from the usual cuboidal γ/γ' configuration to a plate like microstructure [9]. The process is directly controlled by two factors that occur in the early stages of creep deformation: (i) equilibrium interfacial dislocation networks forming at the γ/γ' interfaces and (ii) the γ' particles coalescing by a process of directional coarsening [10]. While the influence of rafting has previously been reported in the uniaxial creep work by Reed et al. [11], its overall effect upon creep life is not fully understood. It is thought rafting may be detrimental at low stresses where creep life may be expected to be long, although it is also considered partially responsible for a creep-hardening effect which initially occurs during testing [10].

Microstructural analysis carried out on post-test SP creep specimens revealed the extent of rafting from each of the experiments and thus helped determine whether the rafting could be considered a temperature or time dependent process. All 1050 °C and 1150 °C specimens developed a fully rafted microstructure, whereas a strong time dependence was found at 950 °C as displayed in Fig. 3. Fig. 4 then shows the SP load vs. time to rupture plot for all of the SP tests performed at each of the temperatures, along with proposed time and temperature dependencies of the rafting regime [12].

The k_{SP} technique, introduced in the EUCoP as a method to correlate conventional and SP creep data [6], was employed to correlate the 950 °C and 1050 °C SP results with those from uniaxial constant load creep tests taken from the literature [12,13]. Fig. 5 plots the stress - time to rupture behaviour for the converted SP tests and the uniaxial constant load creep tests. The k_{SP} was found to differ for the two temperatures (at 950 °C k_{SP} = 0.6, at 1050 °C k_{SP} = 0.8). This difference was attributed to the rafting mechanism which occurred during all of the 1050 °C tests but was limited to the long life tests at 950 °C.

The authors then implemented the Wilshire equations [14] on the combined uniaxial and converted SP data sets at both temperatures, in an effort to predict extended creep lives, in excess of 10,000 h, from the relatively short term creep results. Dislocation processes have been revealed to be the dominant mechanism in creep deformation [15] and previous research had shown the activation energy for diffusion in the γ channels to be 290 kJ mol^{-1} [16]. Nevertheless, an activation energy value of 145 kJ mol^{-1} was determined via the Wilshire plots, where the drop in activation energy was attributed to preferential diffusion paths at higher temperatures [17], although considered more likely due to enhanced freedom of dislocation movement as a result of rafting. The Wilshire predictions based on the 145 kJ mol^{-1} activation energy for 950° and 1050 °C for both the SP and uniaxial creep test methods are reproduced in Fig. 6 [13] On the whole, good agreement is noted between the SP and uniaxial fits at both temperatures, nonetheless, with the uniaxial fits sitting above those of the SP fits. Improved confidence in the appropriate values of activation energy associated with the different microstructural states would benefit future iterations of these predictions.

3.2. γ Titanium aluminides

Small punch creep testing has been applied to a range of γ titanium aluminides [18], intermetallic alloys renowned for their brittle behaviour at room temperature but proven to be relatively

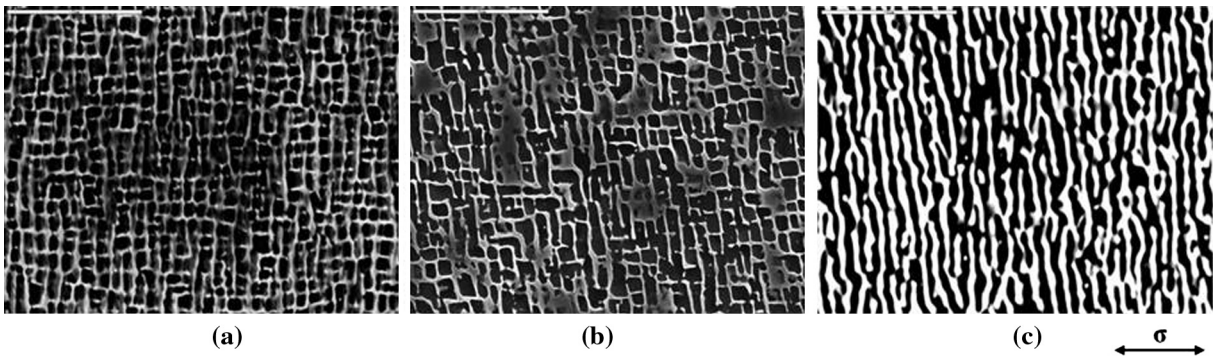

Fig. 3. Evolution of rafting under SP creep testing at 950 °C (a) 350 N, 41 h, (b) 300 N, 105 h, and (c) 250 N, 422 h [12].

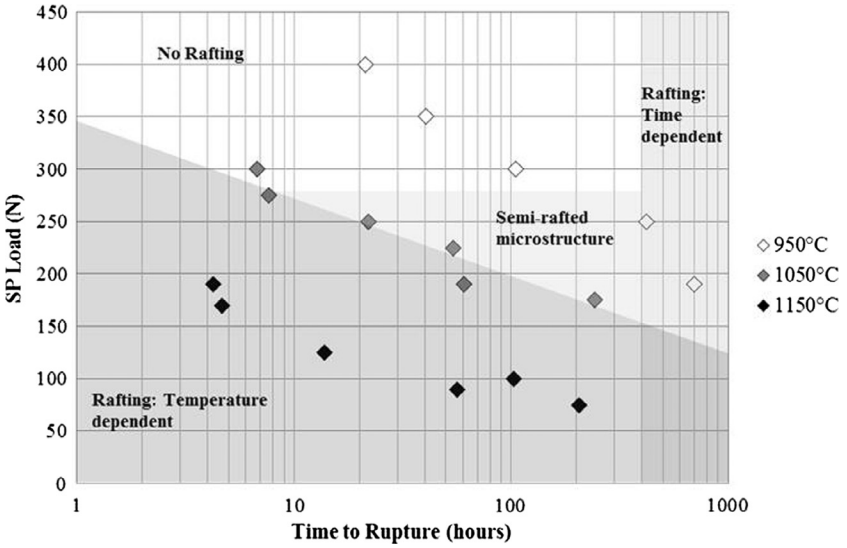

Fig. 4. SP load vs. time to rupture data, along with proposed time and temperature dependencies of rafting [12].

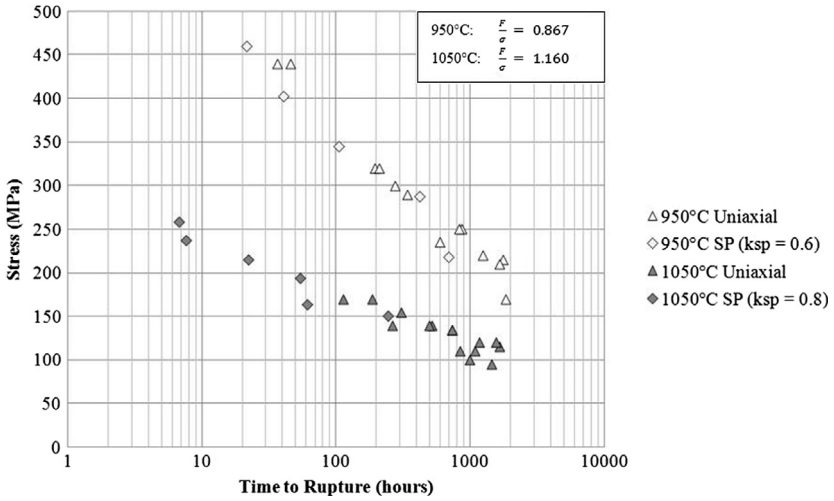

Fig. 5. Stress - time to rupture data for uniaxial constant load creep tests and converted SP creep data at 950 °C and 1050 °C [12].

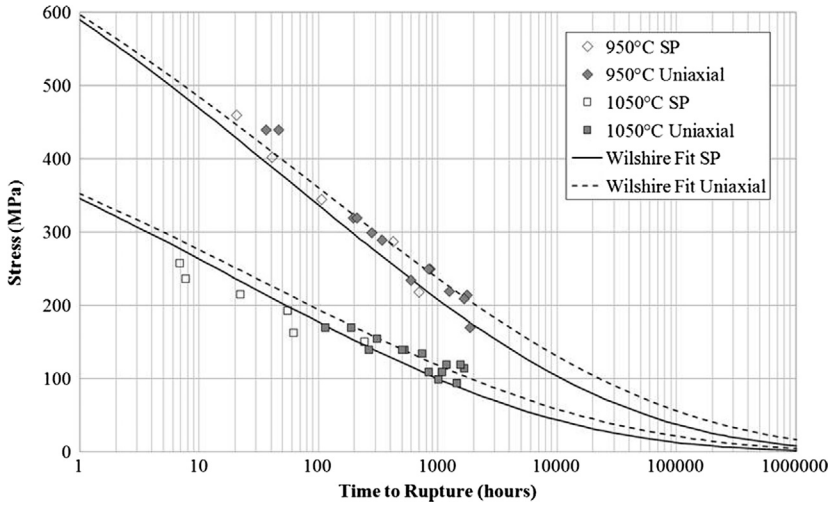

Fig. 6. Wilshire equation predictions of stress-rupture behaviour for CMSX-4® through the SP creep test and the uniaxial creep test [13].

creep ductile at elevated temperatures above 600 °C through conventional test campaigns [19]. Typical displacement–time data from SP tests performed over a range of applied loads define a characteristic creep style response, with a decaying primary stage giving way to a steady state. The onset of tertiary damage under relatively low load/long time conditions was often sudden in nature, Fig. 7. SP testing was sensitive to changes in applied temperature, with differences in strength noted between 700 °C and 750 °C.

Understanding the mechanism of deformation and onset of failure in these SP specimens formed the basis for detailed study. Macroscopic fractures viewed on termination of the test would invariably illustrate a radial cracking pattern, Fig. 8a, distinct from the circumferential failure mechanisms widely noted over many years in ductile materials. The detection of the earliest stages of crack initiation was given particular attention, monitored through a series of interrupted tests on a number of individual specimens. Ultimately, through the use of a servo-mechanical test rig it was demonstrated that radial cracking was induced on the tensile underside of the disc immediately during punch loading, Fig. 8b. Whilst this could be viewed as evidence of a brittle response, from a lifing perspective it is then interesting to note that SP creep specimens subsequently tolerate the presence of this cracking over extended periods of time whilst genuine creep deformation is accumulated.

Finite element modelling was performed to understand the specific stress-strain state imposed during small punch testing of TiAl specimens, Fig. 9. Some success was reported in the prediction of SP displacement–time curves through the FE approach [18], however, the correlation between conventional creep and SP data utilising the K_{sp} technique was less successful for TiAl. The complexity of the small punch test under response to different constitutive properties has yet to receive sufficient attention in the form of modelling.

3.3. IN718 additive structures

With the adoption of additive process techniques for the repair of engineering structures, methods to validate the resulting mechanical properties are required in support of life extension algorithms. To utilise the full potential of the various additive techniques, from the geometric perspective such structures are often complex or encompass thin wall sections. In the aero-engine arena, additive technologies have been focussed upon the localised repair of a variety of chorded rotating aerofoils and static vanes. The relative scale of small punch specimens offers the ability to measure mechanical performance within the boundary of a repair build and depending on section size this may even be possible in all three principal directions. Whenever the volume of the repair is sufficiently extensive, variations in constitutive properties can be measured by careful sampling and extraction of the small punch discs.

This capability has been clearly demonstrated through the deposition of model aerofoil type structures from the workhorse

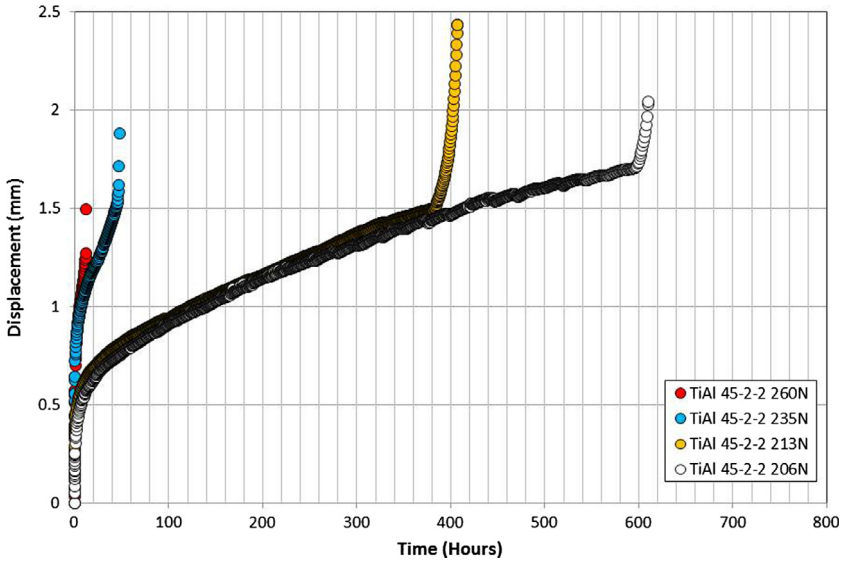

Fig. 7. Typical displacement-time curves measured from TiAl small punch creep specimens tested at 750 °C [18].

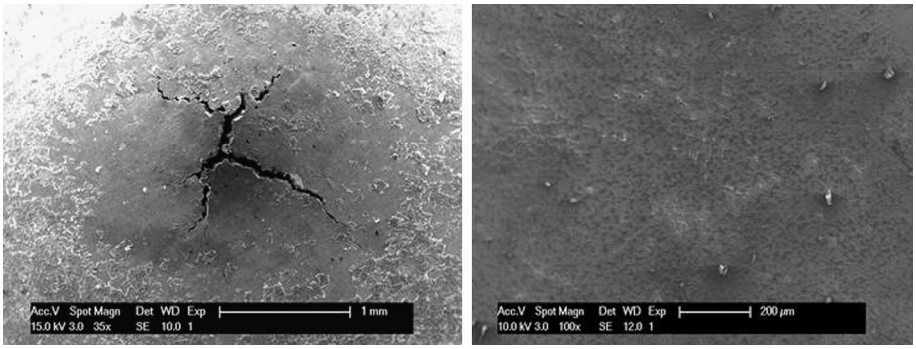

Fig. 8. Cracking under SP testing of TiAl, (a) typical macroscopic radial fractures viewed on termination of test and (b) earliest detected cracking under punch application.

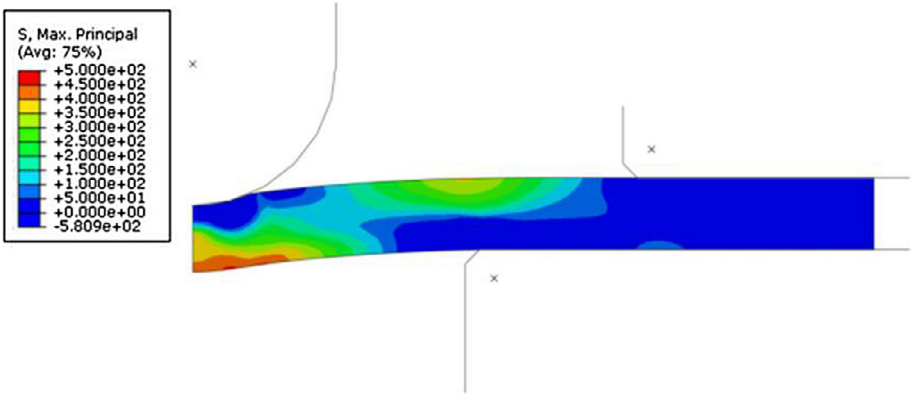

Fig. 9. Finite element modelling of SP creep testing on TiAl [18].

nickel based superalloy IN718 [20]. Without detailed knowledge of the process variables employed to build the structure, it is obvious that the microstructure evolving coincident with the localised deposition of material will be variable, controlled by variations in heat flux as the height of the structure increases relative to the substrate material. For example, standard metallographic techniques can illustrate the typical increase in grain size with distance from the substrate, together with the trend from equiaxed to highly elongated grains, Fig. 10. From classical Hall-Petch theory this would infer differences in strength according to location within the aerofoil. More sophisticated knowledge of the associated variations in micro-texture, however, should also be taken into account. Defining these combined effects on mechanical properties would be difficult employing standard laboratory scale test specimens. However, the small punch technique has been successfully applied in this manner. Discs extracted from different heights in a model aerofoil, Fig. 11, processed via direct laser deposition (DLD) demonstrated a stronger monotonic response near to the DLD/substrate interface compared to mid height and tip regions, Fig. 12. At the same time, the relative performance of the DLD material could be compared to SP results measured from the conventional wrought variant of the alloy.

The small punch specimens also demonstrated the technique's capacity to highlight microstructure and texture control on fracture. Specimens sampling the region close to the substrate, Fig. 13a, failed via characteristic ductile, circumferential cracking. With increasing grain size, grain elongation and stronger texture sampled near the tip of the aerofoil build, failure was typified by a dominant central crack running parallel to the aerofoil build direction, also emphasised in Fig. 13b and c by the prominent thermal etching/oxidation tinting of the surface grain structure during exposure to the test environment at 630 °C.

Where additive structures are built with sufficient scale in three dimensions, discs can be extracted for mechanical assessment in all three principal orientations, Fig. 14. This was reported for IN718 direct laser deposition materials [20]. Whilst similar strengths were measured when loading "across" the build layers (i.e. load applied parallel to the L or T direction), a significantly stronger response was found by loading in the ST direction (in the axis of build epitaxy), Fig. 15, with strength data normalised with reference to the strongest response of any disc specimen.

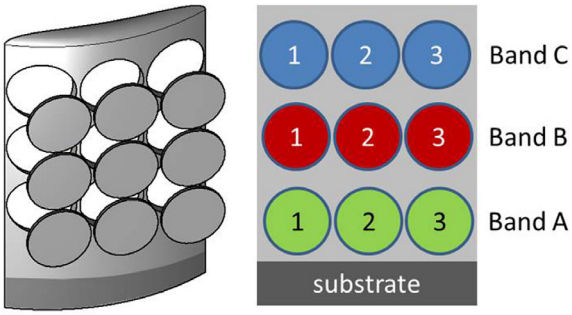

Fig. 11. Small punch disc extraction from a model ALM aerofoil [20].

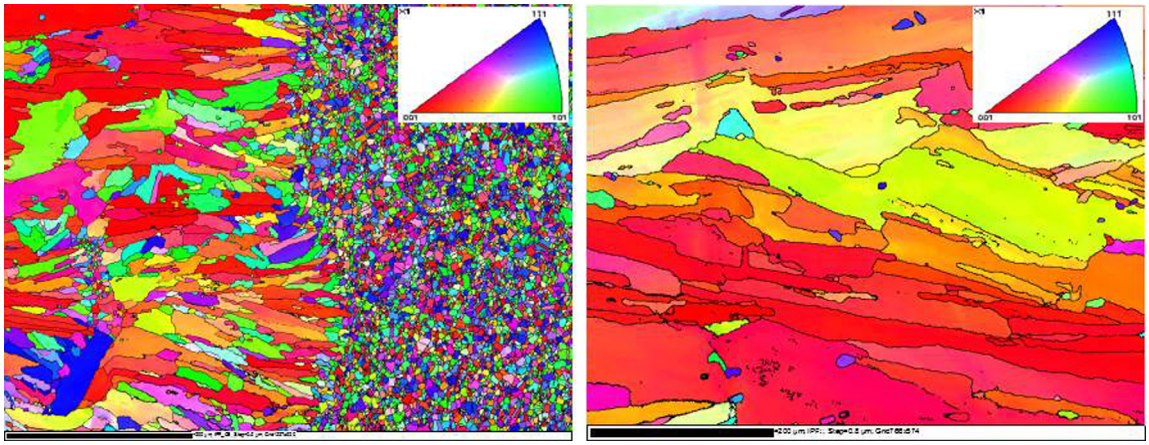

Fig. 10. Variation in grain size and morphology in an IN718 model aerofoil structure, illustrated through EBSD micro-texture maps. (a) substrate-DLD interface and (b) near tip of aerofoil build [20].

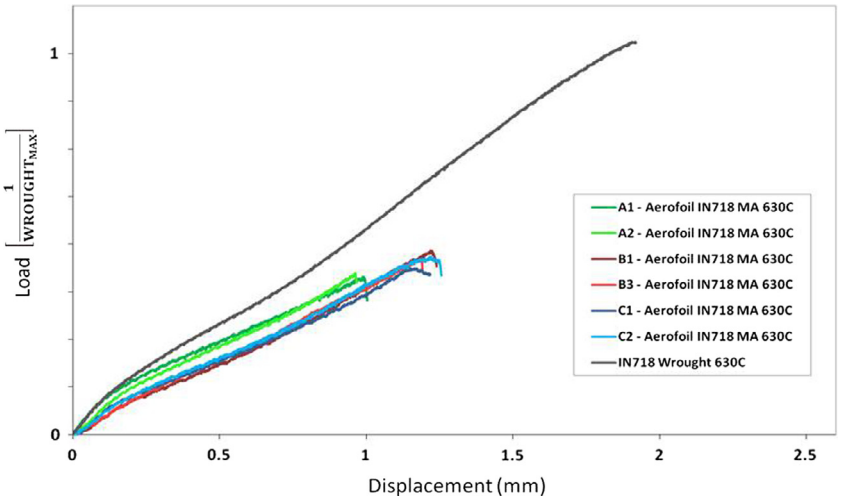

Fig. 12. Small punch tensile response relative to aerofoil build location, with measured load normalised against wrought IN718 response [20].

Detailed relationships with respect to the inherent, columnar, dendritic microstructure were reported.

3.4. Ti-6Al-4V alloys

The SP tensile (SPT) test was adopted to compare the tensile properties of a series of Ti-6Al-4V variants [21], manufactured through a variety of processing routes such as electron beam melting (EBM), cast and hot isostatically pressed (HIP) and traditional forging. The authors performed a number of SP tests on a single material to firstly investigate the influence of displacement rate on tensile performance. Results on the cast & HIP material showed a negligible difference when subjected to a variety of applied displacement rates, covering the range proposed by the EUCoP [6]. The authors attributed any slight variations in properties to similar behaviour seen under uniaxial testing, where both yield stress and ultimate tensile strength is seen to increase with a faster applied strain rate [22]. Following this conclusion, the authors then performed SPT tests at a single displacement rate of 0.6 mm min^{-1} and a temperature of 20 °C to evaluate the constitutive properties of the three Ti-6Al-4V variants.

Fig. 16 demonstrates the change in behaviour across the three materials and suggests that the EBM and cast & HIP variants appear to have a similar response during the initial loading stage to the point where membrane stretching begins. The forged material, however, appears to accumulate a higher proportion of load over this period indicating that this variant exhibits a stronger response. The authors attributed this superior behaviour to the reduced grain size of the forged material, in accordance with the findings of Hall-Petch, with supporting microstructural imaging highlighting the differences.

The specimens also illustrated the level of ductility observed across the three variants where the cast & HIP material experienced approximately 1.57 mm of displacement prior to a 20% drop from the maximum load, whereas the EBM could only accrue 1.28 mm of deformation. This variance is further illustrated in Fig. 17 where fractographic analysis revealed the contrasting failure modes across the three materials. As shown, the cast & HIP material displays fewer dominant cracks and obvious signs of surface plasticity on the tensile underside, consistent with a more ductile response, compared to the EBM disc which fails via a larger number of radial cracks. As such, the SPT test has been shown to be an effective tool for identifying contrasting deformation modes in

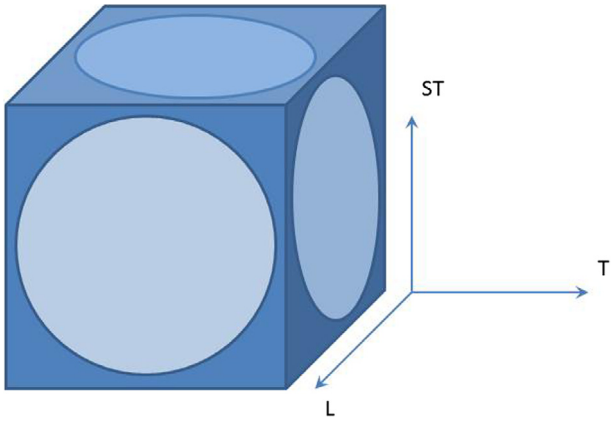

Fig. 14. Disc extraction in three principal orientations relative to a 3D ALM built structure (ST = axis of epitaxy).

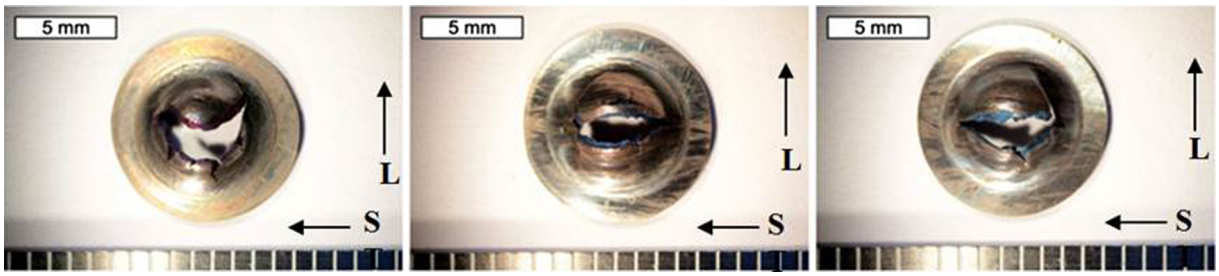

Fig. 13. Fracture morphologies for discs extracted (a) near ALM/substrate interface, (b) mid-aerofoil height, and (c) near aerofoil tip [20].

similar materials, as evidenced by the load-displacement deformation plots and the corresponding fractography for three Ti-6Al-4V variants.

The scale of the SP disc specimens is also beneficial for performing pre and post-test inspections by advanced X-ray computed tomography (XCT), to help identify any processing artefacts which could affect the mechanical performance. Such activity was undertaken by Lancaster et al. [21] on the same materials and whereas two of the Ti-6Al-4V variants (cast & HIP and forged) were found to be 100% fully dense, to a minimum voxel resolution of 6.7 μm, the EBM material contained a number of post processing pores. A thorough investigation was undertaken to characterise these features leading to the conclusion that the porosity did not significantly influence or interact with the crack morphology in this material. However, stress raisers such as sub-surface porosity could potentially have a stronger impact on the mechanical

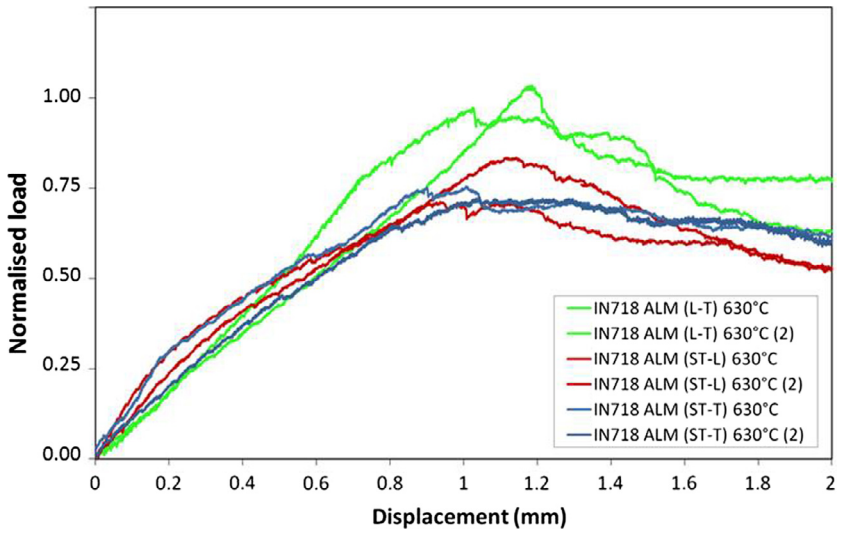

Fig. 15. Small punch tensile response in three orientations relative to an ALM deposit.

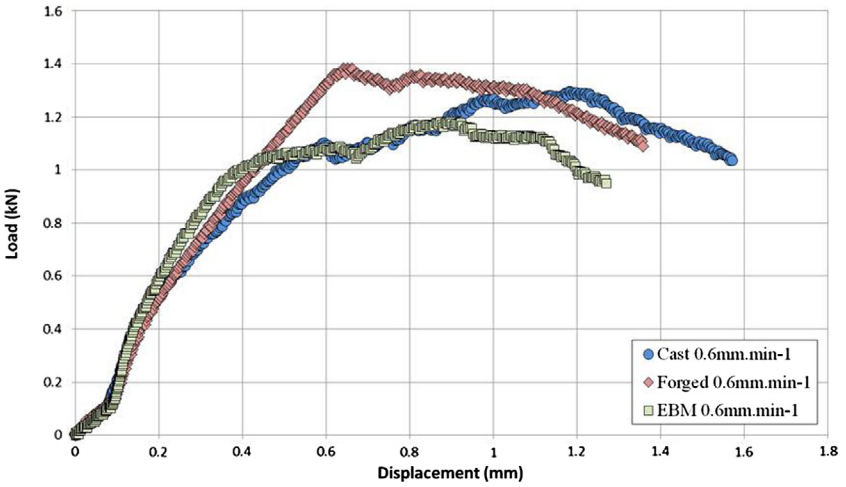

Fig. 16. Small punch tensile behaviour of cast & HIP, forged and EBM Ti-6Al-4V variants at a constant displacement rate of 0.6 mm min^{-1} and test temperature of 20 °C [21].

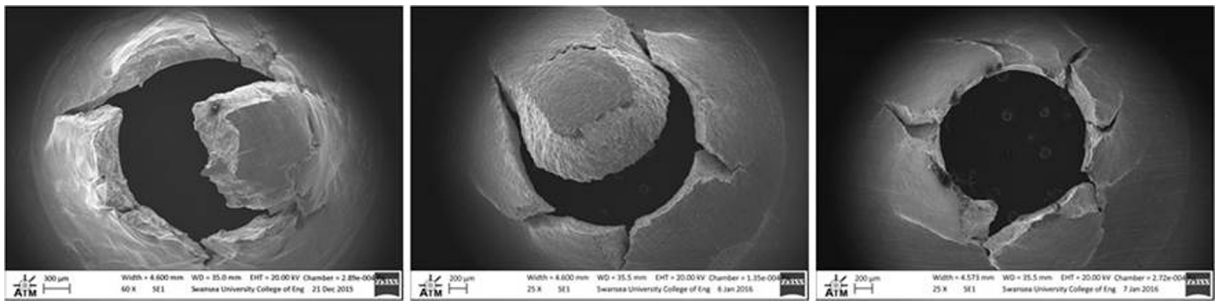

Fig. 17. SEM images of the fractured SP discs for (a) cast & HIP Ti-6Al-4V, (b) forged Ti-6Al-4V and (c) EBM Ti-6Al-4V [21].

response of alternative material systems so the XCT evaluation of SP discs could yet provide a valuable pre-test analysis tool.

4. Conclusions

The aim of this paper was to review a range of programmes carried out in the authors' laboratory to assess materials for application in aero turbine components, in terms of their tensile and creep properties using the small punch testing methodology. Four examples were chosen representing:

(i) a state of the art single crystal nickel based alloy (CMSX-4®)
(ii) a novel intermetallic alloy (γ titanium aluminide)
(iii) IN718 processed via additive layer manufacturing for repair applications
(iv) Ti-6Al-4V also processed by additive layer manufacturing for full scale component manufacture

Small punch techniques have proven invaluable as an evaluation tool towards alloy development, mainly through their ability to rank materials from relatively small material stocks. They provide particular benefits during the development stages for additive processing, whilst optimising process parameters and alloy compositions, including the ability to characterise mechanical performance in three dimensions.

Acknowledgements

The current research was funded under the EPSRC Rolls-Royce Strategic Partnership in Structural Metallic Systems for Gas Turbines (grants EP/H500383/1 and EP/H022309/1). The provision of materials and supporting information from Rolls-Royce plc is gratefully acknowledged by the authors together with the assistance provided by Tomas Garcia, Gregg Norton, Will Harrison, Robert Owen, Rajiv Banik, Henry Illsley and Gareth Davies in completing the experimental work and modelling simulations. Mechanical tests were performed at Swansea Materials Research and Testing Ltd. (SMaRT). Requests for access to the underlying research data should be directed to the corresponding author and will be considered against commercial interests and data protection.

References

[1] M.P. Manahan, A.S. Argon, O.K. Harling, The development of a miniaturized disk bend test for the determination of postirradiation mechanical properties, J. Nucl. Mater. 104 (1981) 1545–1550, http://dx.doi.org/10.1016/0022-3115(82)90820-0.
[2] J. Kameda, X. Mao, Small-punch and TEM-disc testing techniques and their application to characterization of radiation damage, J. Mater. Sci. 27 (1992) 983–989, http://dx.doi.org/10.1007/BF01197651.
[3] T. Izaki, T. Kobayashi, J. Kusumoto, A. Kanaya, A creep life assessment method for boiler pipes using small punch creep test, Int. J. Press. Vessel. Pip. 86 (2009) 637–642, http://dx.doi.org/10.1016/j.ijpvp.2009.04.005.
[4] F. Di Persio, G.C. Stratford, R.C. Hurst, Validation of the small punch test as a method for assessing ageing of a V modified low alloy steel, in: Balt. vi Life Manag. Maint. Power Plants, 2004, pp. 523–535.
[5] J.S. Ha, E. Fleury, Small punch tests on steels for steam power plant, KSME Int. J. 12 (1998) 818–835.
[6] CEN Workshop Agreement CWA 15267, European Code of Practise: Small Punch Test Method for Metallic Materials, 2007.
[7] P. Caron, Y. Ohta, Y.G. Nakagawa, T. Khan, Creep deformation anisotropy in single crystal superalloys, Superalloys (1988) 215–224.
[8] C. Knobloch, S. Volker, D. Sieborger, U. Glatzel, Anisotropic creep behavior of a nickel-based superalloy compared with single phase nickel solid solution and y' phase single crystals, Mater. Sci. Eng. A. 237–241 (1997).
[9] A. Royer, P. Bastie, M. Veron, In situ determination of γ′ phase volume fraction and of relations between lattice parameters and precipitate morphology in Ni-based single crystal superalloy, Acta Mater. 46 (1998) 5357–5368, http://dx.doi.org/10.1016/S1359-6454(98)00206-7.
[10] R.C. Reed, The Superalloys: Fundamentals and Applications, Cambridge University Press, USA, 2006.
[11] R.C. Reed, N. Matan, D.C. Cox, M.A. Rist, C.M.F. Rae, Creep of CMSX-4 superalloy single crystals: effects of rafting at high temperature, Acta Mater. 47 (1999) 3367–3381, http://dx.doi.org/10.1016/S1359-6454(99)00217-7.
[12] S.P. Jeffs, R.J. Lancaster, Elevated temperature creep deformation of a single crystal superalloy through the small punch creep method, Mater. Sci. Eng. A. 626 (2015) 330–337, http://dx.doi.org/10.1016/j.msea.2014.12.085.
[13] S.P. Jeffs, R.J. Lancaster, T.E. Garcia, Creep lifing methodologies applied to a single crystal superalloy by use of small scale test techniques, Mater. Sci. Eng. A. 636 (2015) 529–535, http://dx.doi.org/10.1016/j.msea.2015.03.119.
[14] B. Wilshire, A.J. Battenbough, Creep and creep fracture of polycrystalline copper, Mater. Sci. Eng. A. 443 (2007) 156–166, http://dx.doi.org/10.1016/j.msea.2006.08.094.
[15] M.T. Whittaker, B. Wilshire, Advanced procedures for long-term creep data prediction for 2.25 chromium steels, Metall. Mater. Trans. A. 44 (2012) 136–153, http://dx.doi.org/10.1007/s11661-012-1160-2.
[16] J. Svoboda, P. Lukis, Activation energy of creep in [0 0 1]-orientated superalloy CMSX-4 single crystals, Mater. Sci. Eng. A. 234–236 (1997) 173–176.
[17] R.W. Evans, B. Wilshire, Introduction to Creep, The Institute of Materials, Swansea, 1993.
[18] R.J. Lancaster, W.J. Harrison, G. Norton, An analysis of small punch creep behaviour in the γ titanium aluminide Ti–45Al–2Mn–2Nb, Mater. Sci. Eng. A. 626 (2015) 263–274, http://dx.doi.org/10.1016/j.msea.2014.12.045.
[19] Z. Abdallah, M.T. Whittaker, M.R. Bache, High temperature creep behaviour in the γ titanium aluminide Ti–45Al–2Mn–2Nb, Intermetallics 38 (2013) 55–62, http://dx.doi.org/10.1016/j.intermet.2013.02.003.
[20] R.J. Lancaster, R. Banik, R.C. Hurst, M.R. Bache, G. Baxter, Application of small punch test methods to advanced manufactured structures, in: 3rd Int. SSTT Conf. Determ. Mech. Prop. Mater. by Small Punch Other Miniat. Test. Tech., Schloss Seggau Seggauberg, 2014, pp. 170–178.
[21] R.J. Lancaster, G. Davies, H. Illsley, S.P. Jeffs, G. Baxter, Structural integrity of an electron beam melted titanium alloy, Materials (Basel) 9 (2016), http://dx.doi.org/10.3390/ma9060470.
[22] S. Tammas-Williams, H. Zhao, F. Léonard, F. Derguti, I. Todd, P.B. Prangnell, XCT analysis of the influence of melt strategies on defect population in Ti-6Al-4V components manufactured by Selective Electron Beam Melting, Mater. Charact. 102 (2015) 47–61, http://dx.doi.org/10.1016/j.matchar.2015.02.008.